Test Demonstrated Damage Tolerance of F-22 Wing-Attach Lugs with ForceMate™ Bushings

M. Cayton, J. Bunch, P. Walker
Boeing Integrated Defense Systems

J. Brown, T. Brussat
Lockheed Martin Aeronautical Systems

J. Ransom, T. Poast
Fatigue Technology, Inc

W. Garcia, R. Bair
478th Support Wing, USAF

Background

The F-22 aircraft design was subjected to a full scale fatigue test to demonstrate the capability of the design and overviews of this test have been previously presented (References 1 and 2). Keeping with the requirements of most full scale structural tests conducted by the U.S. Air Force, a complete teardown of the tested airframe was conducted after the test was completed. The purpose of the teardown was to identify any cracking or other anomalies that had remained undiscovered after completion of testing.

One such structural detail where a crack was discovered after the test was completed was one of the wing attachment lugs. The wings of the F-22 are attached to the aircraft by 6 pairs (per side) of lugs in an upper/lower configuration hence there are 12 lugs per side for a total of 24 wing attach points. The lower lugs are the most critical for durability and damage tolerance (DADT) as they react the wing up-bending loads in tension. During teardown, and after 2.5 lifetimes of testing, a crack was discovered on each lower lug at the STA657 attach point on opposite sides of the aircraft. These same lugs each experienced cracking at nearby lower profile locations that required repairs during the test. Figure 1 (taken from reference 2) shows the location of the cracks associated with the lug. During correlation of the lug bore crack(labeled as crack 2 in Figure 1), it was hypothesized that the crack at the lower lug profile (labeled as crack 2 in Figure 1) influenced the nucleation of the crack at the lug bore.

Figure 2 shows the bore crack found on the left hand side of the test aircraft. The crack shown in Figure 2 was the larger of the two lug bore cracks; however, the crack on the right hand side was also visually detectable. Prior to completion of the test, the test article, including the cracked lugs were subjected to full limit load so there was no question that the lugs continued to function as load carrying members for the full 2.5 lifetimes of testing, and correlation of the cracks to analysis indicated that the lug met full durability life requirements. The crack growth correlation analysis did result in additional damage tolerance inspections due to the possible occurrence of a rogue flaw.

There were circumstances associated with the test article supporting a conclusion that the cracking was actually an anomaly of the testing. Specifically, evidence supporting the cracks as anomalous included

- Close proximity to repairs made during the course of the fatigue test
- Cracking occurred at only one station even though the nominal stresses in each lug were approximately equal
- The lower lug pins at STA657 seized during the course of the test which allowed for significant wing bending moment to be transferred through the pin joint

Conversely, one fact disputed the notion that the cracks were anomalous, specifically

- Symmetric cracks were observed on both the left and right hand sides of the test aircraft.

The inspections that resulted from damage tolerance correlation required removal of the wings to get access to the critical area each time an inspection was required, and since this added an unplanned level of complexity to aircraft maintenance. Since the requirement to revomve the wing was significant, and there were possible compromising issues with the full scale fatigue test, a component test program was launched to verify the damage tolerance life of the lower lug. The objectives of the test program were to

- Address the possibility that the observed full scale test cracking was an anomalous result
- Extend inspection intervals for the lugs where full scale fatigue cracking was observed
- In conjunction, with the 2nd item, develop the empirical database to establish the crack growth life improvement obtained with an interference fit bushing of the scale required for this lug

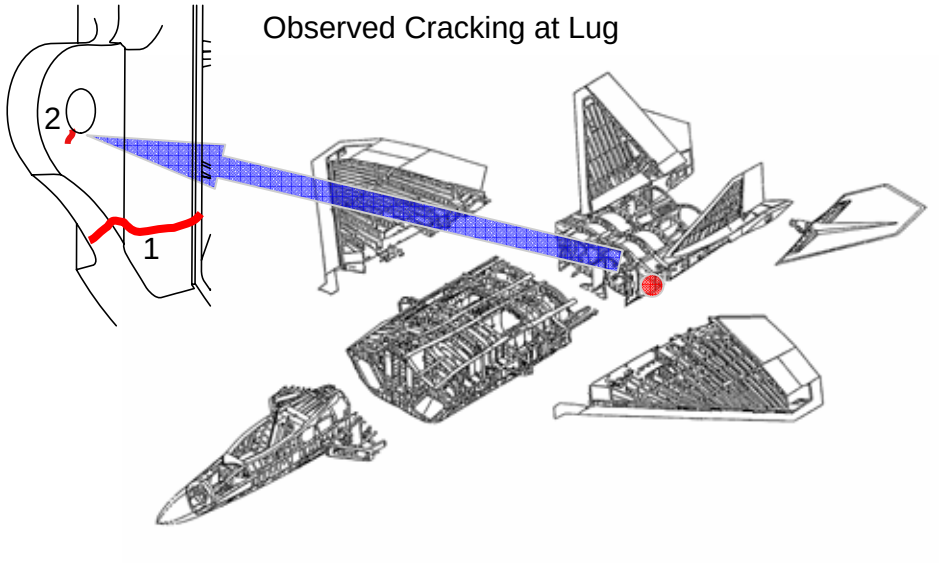

Figure 1 Cracking at frame lug. Location 1 discovered and repaired at approximately 1.2 lives. Location 2 discovered at teardown after 2.5 lives.

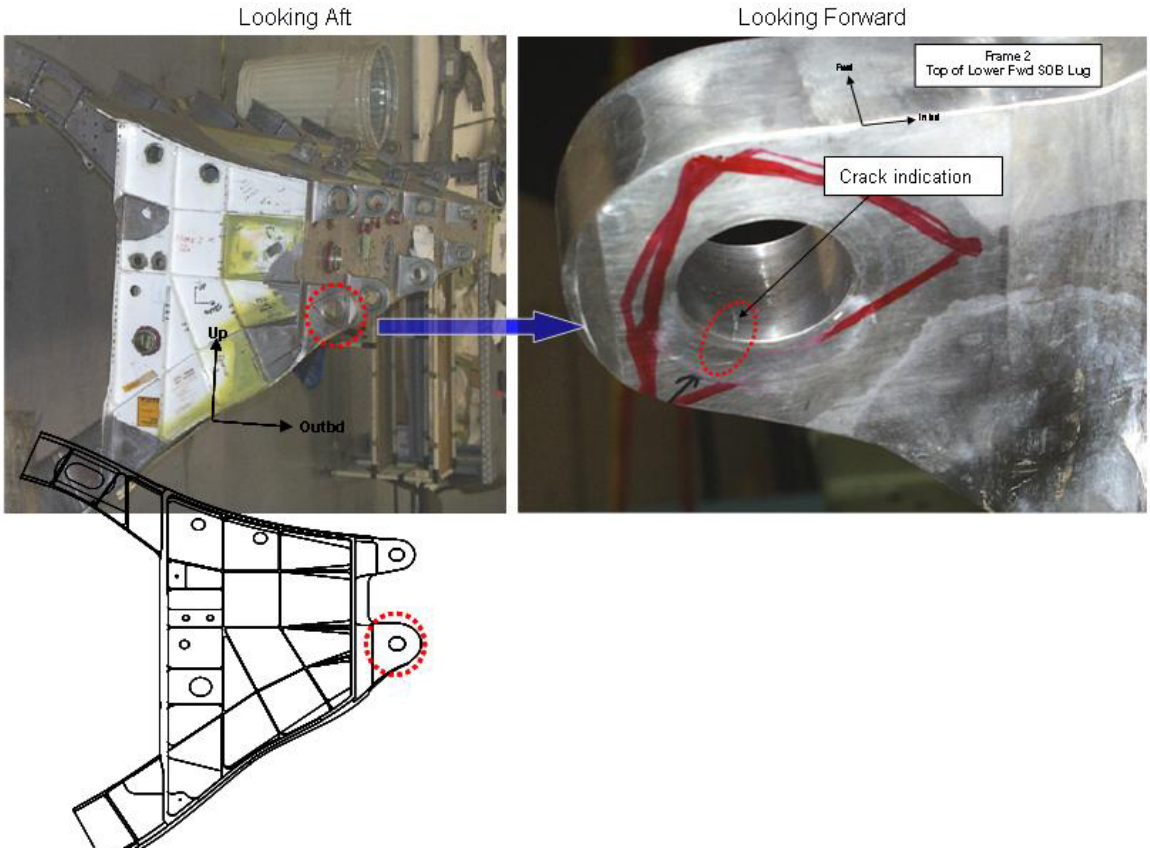

Figure 2 Location of cracking observed on lug bore, left hand side shown, smaller crack at similar location observed on right hand side.

A total of 9 specimens were tested and the specimens are listed by Specimen ID in Table 1., This table also summarizes the key test variables associated with each specimen. For the specimens discussed in this work, the material, load spectra, and overall geometry were identical. The key variables investigated were

- Bushing expansion, a net fit bushing and two ForceMate bushings with different expansion levels were tested
- Notch location, as will be discussed in the following sections, affected test results and two notch configurations were tested as part of this investigation.

All specimens listed in Table 1 were machined from Ti-6Al-4V forgings. The forgings were obtained from Wyman Gordon and had been processed and heat treated following the same specifications as the aircraft components. The forgings were heat treated by beta annealing followed by an overaging solution treat anneal. The resulting microstructure was a coarse grain structure of prior beta grains with alpha-beta colony laths.

Figure 4 is a diagram showing the specimen design and the applied load vector. When the specimen is loaded into a uni-axial test frame, the applied load aligns through the center of each of the lug holes. From Figure 4, it is clear that the specimen is a double lug, and this design made the specimen a self aligning specimen with the added benefit of making the specimen easy to configure into the test frame. These features of the specimen facilitated the test procedure since the specimen was removed from the test frame in order to make the crack growth measurements.

Close inspection of Figure 4 reveals that each of the lugs on either end are different sizes. This was an intentional feature of the specimen design. By making one lug slightly larger, this eliminates the chances of failure at a region that was not part of the specimen design. The pocket machined between the two lugs was designed to tailor the actual stress profile at the test location to be representative of the actual aircraft. The sketch of the specimen shows a bushing at the lug bore. Two types of bushings were used for this investigation:

- Net fit bushing of a copper bronze material
- ForceMate® bushing of a Cu-Be (copper beryllium) alloy

The ForceMate® system (Fatigue Technology Inc, Seattle) involves the cold expansion of an initially clearance fit bushing into a hole. A specially sized bushing, with a proprietary lubricant on the inside surface, is radially expanded into the hole using a tapered expansion mandrel. The process of expanding the bushing will yield it into the hole creating a high interference fit. Depending on the combination between the bushing material and the parent material, the installation process may also cold expand the base material inducing beneficial residual compressive stresses. In addition to providing a rapid, more consistent, and non-damaging bushing installation, the high interference fit and possible cold expansion of the parent material will result in an installation that will resist bushing rotation/migration and have a greatly enhanced fatigue life. The complete ForceMate process is shown in Figure 3.

Figure 3 Description of ForceMate® process

A primary objective of this investigation was to understand the level of crack growth life benefit that was obtained from the ForceMate® process when applied to lugs of this scale, and as part of this investigation two expansion levels were tested.

Table 1 Summary of specimens tested

Specimen ID	Bushing Variables	Notch Location	Test Objective
B-K-SP	Net Fit	64.3°	Baseline crack growth data for lug geometry and loading
A-K-SP	Net Fit	64.3°	Baseline crack growth data for lug geometry and loading
B-LL-3	ForceMate, Original expansion	64.3°	Test Capability of the original design ForceMate Bushing
A-UL-2	ForceMate, Original expansion	64.3°	Test Capability of the original design ForceMate Bushing
A-LL-1	ForceMate, Original expansion	64.3°	Test Capability of the original design ForceMate Bushing
B-UK-6	ForceMate, Orignal with Lowest applied Expansion	72.0°	Test for lowest expansion within specification tolerances of the original design
A-UK-5	ForceMate,Original Expansion	72.0°	Test for the original design bushing configuration
B-LK-7	ForceMate, Increased Expansion	72.0°	Test for capability of an increased expansion bushing
B-UL-4	Test started with Original Expansion, replaced by ForceMate, Increased Expansion at 0.5 lifetime	64.3°	Test the feasiblity of getting crack growth life improvement by retrofitting the original bushing with the increased expansion
Orientation of notch is shown in Figure 8. Orientation of 64.3° corresponds to the location of cracking observed on the full scale fatigue test, while 72.0° corresponds to the location of the peak stress			

When the specimen is placed into a uni-axial test frame, the specimen aligns such that the vector goes through the center of each lug as shown in Figure 4. The coordinate system shown next to the diagram of the lug shows the loading on the specimen relative to the aircraft coordinates. Positive F_y and F_z loads as shown on the coordinate system in Figure 4 load the specimen in tension, and the net resultant would be at the angle relative to the horizontal axis. For spectrum loading, careful consideration was given to the actual load vector angle that should be applied to the test specimen. With two load actuators, it would have been possible to control both load axes independently, but as previously mentioned, one of the test constraints was to perform the test in a uni-axial test frame. Figure 5 is a photograph of the test setup and also shows a diagram of the specimen rotated as it appears in the test setup photograph.

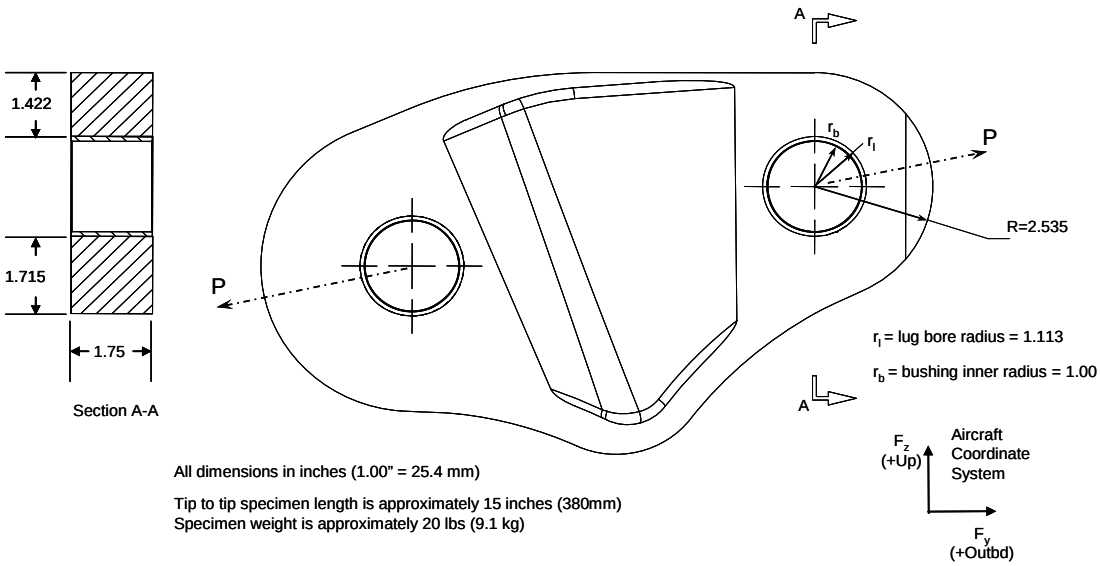

Figure 4 Configuration of lug test specimen with applied load vector to represent aircraft loading. The lug on the right side of the diagram is the test section.

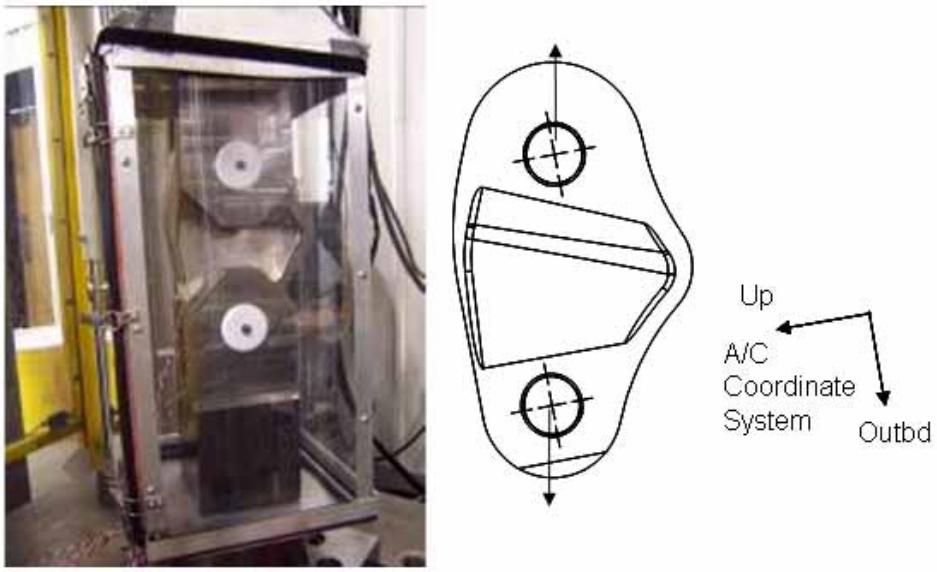

Figure 5 Test specimen aligned in test frame, photograph on the left is picture of test setup.

To confirm that a representative test could be designed and performed with a single load axis, the F_y and F_z load components for each of the fatigue load conditions in the test spectrum were plotted on Cartesian coordinates. Such a plot is used to establish if there is a correlation between the two load components. Figure 6a shows that when these load conditions are plotted, there is a tight correlation about a straight line indicating that the F_y and F_z load components are not independent, i.e. the magnitude of the F_z load is itself dependent on the magnitude of the F_y load. The resultant load angle for each of the load conditions was computed and a histogram of the angles (Figure 6b) demonstrates that predominantly, the majority of the loads occur at a resultant angle between 10 and 20 degrees.

For spectrum loading of the lug specimen, the load angle for the design reference condition (i.e. the maximum spectrum load) was determined to be 11.5 degrees, and each of the other load

cases making up the fatigue spectrum was rotated to this angle. Figure 6a shows many points on the plot where both Fy and Fz are negative, the resultant of which would result in a compressive load on the specimen. The double lug specimen is not suitable for fully reversed loading that includes compression cycling. This is not a limitation, since lugs are critical for tension loading and compressive cycles do not load the critical area of interest for these tests. Hence all compression loads were clipped from the spectrum. The exact clipping level was about 5% of the maximum load. Clipping slightly above zero allowed for uncertainty in the controller of the servohydraulic test frames.

Two final spectrum manipulations were made to the final test spectrum, the test spectrum was subjected a range truncation, to eliminate small load reversals that did not contribute significantly to fatigue damage, and finally, all peak loads were bumped by 9.06% to account for additional tension loading that is applied to the actual aircraft resulting from friction between the pin and bushing surfaces. This friction is due to rotation of the joint on the aircraft and results in a moment that has the effect of increasing the tension load at the critical location. Exceedance curve comparisons of the test spectrum before clipping and truncation and the final test spectrum are shown in Figure 7.

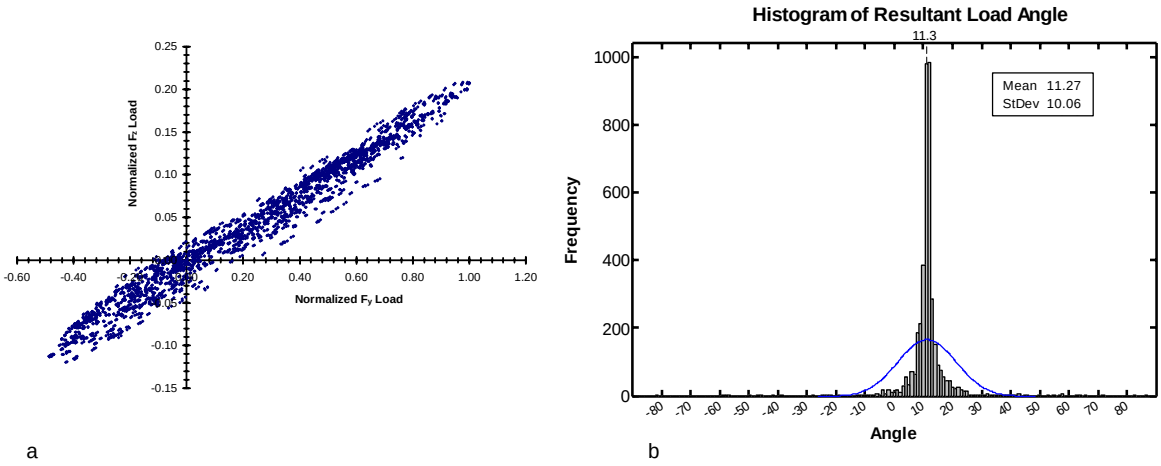

Figure 6 (a) Plot of Fy fatigue spectrum loads vs. F_z loads. All loads are normalized to max F_y load. (b) Histogram of resultant load angle, showing predominance of load vector angle between 10 and 20 degrees

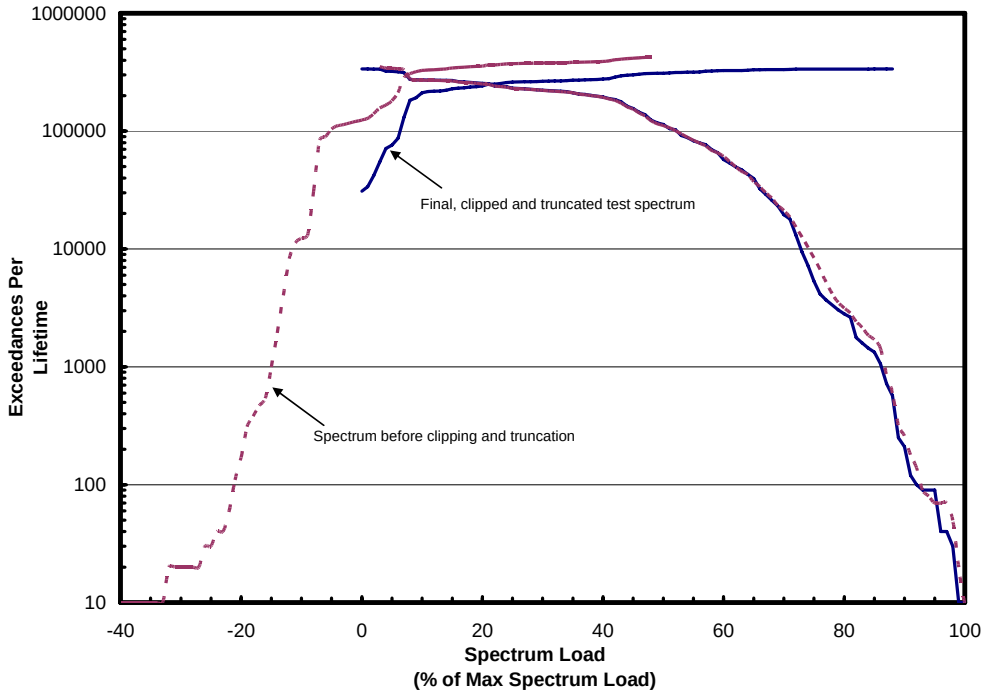

Figure 7 Exceedance plot for applied test spectrum.

Two servo-hydraulic test frames were used for all tests discussed in this work. One frame was had a capacity of 600 Kips the second had a capacity of 500 kips. The maximum spectrum load applied to any of the specimens was 247 kips. The spectrum created for this test represented one-tenth of a lifetime of aircraft usage. The effective cycling rate applied to the specimen was about 0.33 cycles per second, and at this rate it took about 11 hours to complete one 0.10 lifetime spectrum block.

Because the clevis of the test frame fixture used to grip and load the specimen obscured the critical area of the specimens, it was not possible to measure crack growth *in situ*. The specimen was removed from the test frame to measure the crack length. The frequency of crack measurement typically started out at once every 0.2 lifetimes and increased in frequency as the test progressed in order to get as much definition as possible of the crack growth curve. Crack growth measurements were made by placing the specimen onto a metallurgical microscope capable of quantitative length measurements. The total crack length from the tip of the EDM notch was recorded at every measurement interval.

The objective of the test program was to obtain crack growth data with specimens having ForceMate® bushings installed, and therefore, it was necessary to give careful consideration to the process of inducing a preflaw into the specimen. Since these were damage tolerance tests, the condition being tested simulates the possibility of a rogue flaw being present at the worst possible location. Two flaw locations were tested in this investigation; the first specimens tested had the EDM notch placed at a location corresponding to the orientation of the cracks observed on the full scale fatigue test, and for reasons to be discussed in the next section, it was necessary to relocate the notch on subsequent tests in order to obtain crack growth data. Figure 8 shows the relative location of the EDM notches to each other and the orientation of the notches on the lug specimen.

An EDM notch is not a sharp crack, so before starting the test, the specimens were pre-cracked. The following steps summarize the process of inducing a pre-crack into the specimen:

- The specimen was machined with the bore diameter undersized by 0.02 inches
- An EDM notch was cut into the specimen at the desired location the length of the notch geometry replicated a corner flaw 0.03 inches on the surface of the lug by 0.03 inches into the bore.
- A temporary net fit bushing was installed
- The specimens were subjected to constant amplitude cycling at an R-ratio of 0.05.
- Crack length from the notch was monitored during constant amplitude cycling. The target maximum crack length was 0.06 inches.
- The temporary bushing was removed and the hole was reamed to final size
- The final bushing was installed and the specimen was ready for test

This process replicates the scenario of a rogue flaw present at the time the bushing was installed into the lug, and by following these steps, a crack-like defect approximately 0.045 to 0.050 inches in size was placed into the specimen at the time of manufacture. Having a true crack like defect also provided for the most conservative test and most closely represented the analytical case.

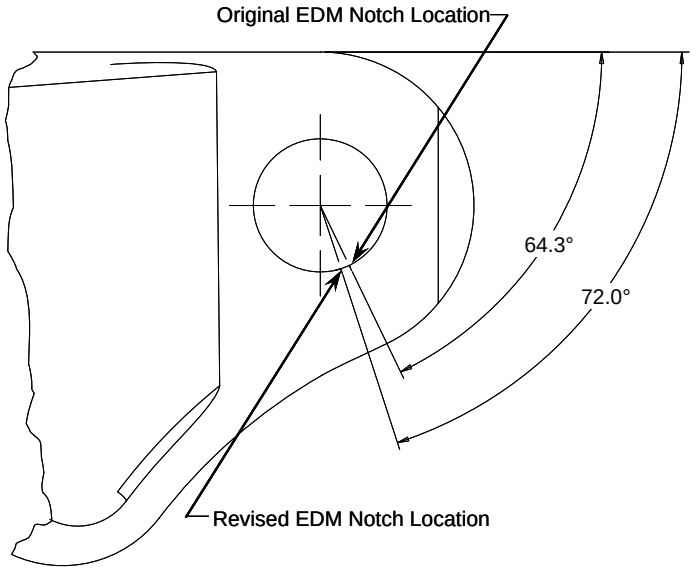

Figure 8 Location of EDM notches used to initiate the crack. The original specimen design had the EDM notch at the precise orientation as the cracking on the full scale fatigue test.

Experimental Strain Analysis

In addition to fatigue tests, a specimen was strain gauged to understand the level of strain applied during installation of the ForceMate bushings. The objective of this aspect of the investigation was to obtain experimental verification of the strain levels in the specimen during installation and residual tension stress levels on the outer perimeter of the specimen. This specimen was also used to determine the changes in residual strain after reaming the bushing to final diameter.

For the experimental strain analysis specimen a lug profile identical to the test section of the fatigue specimens was machined from a 7” by 7” (178mm x 178mm) square block of Ti-6Al-4V Beta annealed titanium processed to the same specifications as the fatigue specimen material, and this specimen was instrumented with 11 strain gages. Eight of these gages (EP-08-015DJ-120) were installed on the front and back surfaces of the part. These gages recorded the hoop strain during the expansion of the hole. Three gages (CEA-05/06-125UN-350) were installed on

the edge of the part. The gage locations are shown in Figure 9 and correspond to critical locations on fatigue test lug. The gages were bonded to the specimen using M-Bond 200 adhesive with a room-temperature cure, and to protect the gages after installation, they were coated with M-Coat A. All strain gage supplies were from Vishay Micromeasurements, Raleigh, NC.

The bushing was installed into the test part using the FTI ForceMate® process. Teflon® was inserted between the installation tooling and the surface of the lug during installation to protect the strain gages from the bushing installation tool. A washer of the same inner and outer diameter of the bushing was used to compensate for the offset created by the use of the Teflon and to ensure bushing flushness was maintained. The strain gages were connected to Vishay 2150 strain gage conditioners, a LabView software package was used to process the data. During installation of the bushing, the eight surface gages were monitored with data acquisition throughout the processing. For the three edge gages, only the residual strain after bushing installation was recorded.

The bushing was reamed after installation to the identical diameter as the fatigue test lug. The gages were reconnected to the Vishay rack and zeroed prior to the start of reaming. The bushings were reamed in progressive steps due to manufacturing considerations. Strain gage readings were recorded before and after each iteration of the reaming process.

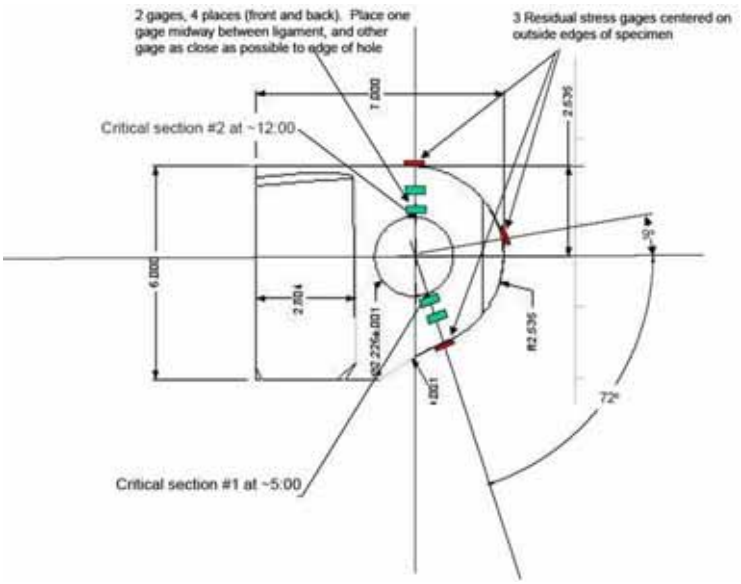

Figure 9 Strain gage layout for expeimental strain analysis of busihng installation

Experimental Results (make more prominate change from setup section to results section)

The specimens in Table 1 can be grouped into 3 general configurations regarding the type of bushing installed, and the discussion of the test results will group the results accordingly:

- *"Net Fit",* a slight shrink fit bushing with just enough interference to keep the bushing in place during testing. Even though there is a slight interference, these bushings are referred to as "net fit" bushings in this work. These specimens were the controls providing reference data with which to gage the level of life improvement obtained from higher interference fit bushings.

Table 2 Summary of Test Results

Specimen ID	Bushing	Notch Location	Life to Failure	Test Result
B-K-SP	Net Fit	64.3°	1.15	*Failed due to crack growth from induced pre-flaw*
A-K-SP	Net Fit	64.3°	1.01	*Failed due to crack growth from induced pre-flaw*
B-LL-3	Current	64.3°	2.08	*Failed due to initiation of secondary cracks in the lug bore*
A-UL-2	Current	64.3°	*2.47*	*Failed due to initiation of secondary cracks in the lug bore*
A-LL-1	Current	64.3°	3.11	*Failed due to initiation of secondary cracks in the lug bore*
B-UK-6	Current	72.0°	*1.51*	*Failed due to crack growth from induced pre-flaw*
A-UK-5	Current	72.0°	*1.44*	*Failed due to crack growth from induced pre-flaw*
B-LK-7	Revised	72.0°	*>10.7*	*Multiple small cracks initiated but none grew significantly. Only a small amount of growth was noted from the EDM pre-flaw*
B-UL-4	Revised*	64.3°	*>8.9*	*Multiple small cracks none grew significantly Initial pre-crack grew from 0.05 in to 0.13 in. Most growth was during first 0.5 lifetime*

* B-UL-4 had a current configuration bushing installed for the first 0.5 lives of testing. This bushing was then removed and replaced with a revised configuration.

- *"Current", ForceMate* bushings with the applied using current F-22 specifications that represented the fatigue test. These specimens provided the data to establish the capability of the lugs with bushings installed to the current configuration.
- *"Revised", ForceMate* bushings with interference levels increased beyond current specifications to test the feasibility of gaining additional life improvement benefit over the current installations. These tests included one specimen with the revised bushing installed at the beginning of the test, and one specimen that started testing with a current configuration bushing that was removed and replaced with the revised bushing at one-half lifetimes. This tested the feasibility of retrofitting current bushings with new bushings.

Table 2 lists the results summary as total life to failure and also lists the dominant failure mode. The summary in Table 2 shows that the specimens with the net fit bushing had the shortest life to failure. For the specimens with the original interference fit bushings, there was a distinct effect of the EDM notch orientation. Whereas, for the increased expansion bushing, the growth of the EDM induced cracks as well as naturally nucleated cracks was effectively suppressed for both orientations.

The primary objective of these fatigue tests was to collect data on the growth of cracks growing from induced flaws, the test results also provided opportunities to gain insights on the failure modes of titanium lugs with Cu-Be bushings installed.

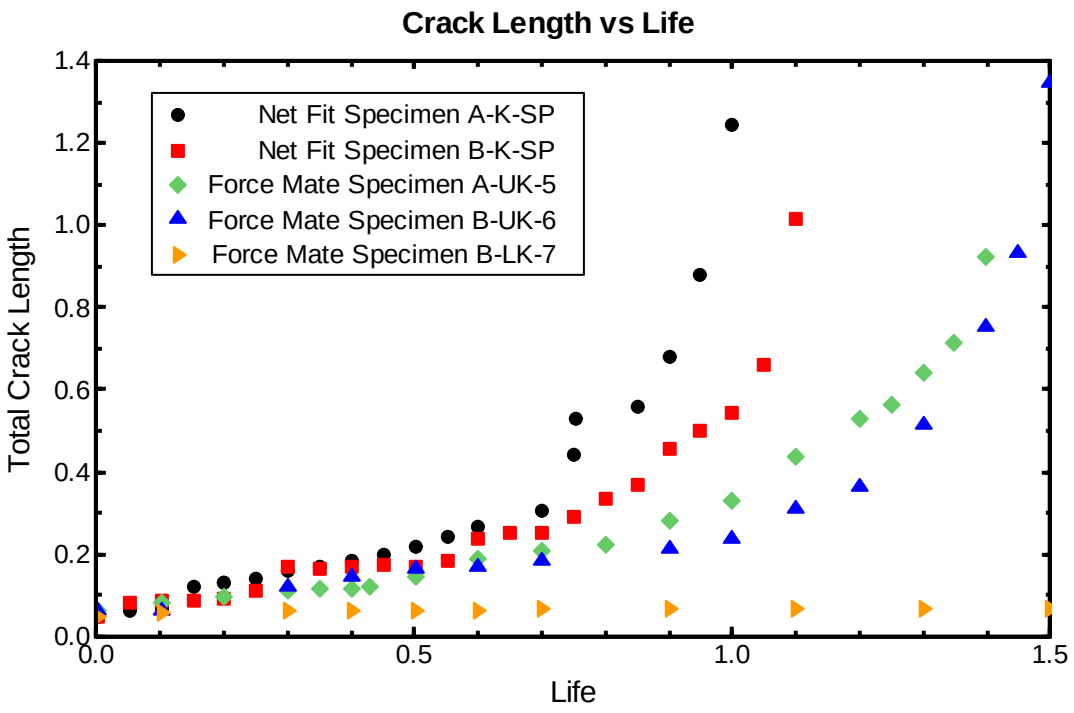

Figure 10 Test results plotted as crack length vs spectrum fatigue life

Net Fit Bushing Results

The results of the net fit bushing tests are presented in Figure 10 as a plot of crack length vs Spectrum lifetime. The test results for both A-K-SP and B-K-SP are both very repeatable when plotted in this manner and the fracture surfaces of these specimens were typical for a coarse grain titanium alloy. Most notably, failure occurred by a crack growing from the induced pre-flaw. Ultimately the specimens failed in net section yield.

The results from the net fit bushing tests provided confidence in the specimen design and the overall test procedure. The results for specimens A-K-SP and B-K-SP plotted in Figure 10 provide the reference data by which to judge the benefit of the interference fit bushing tests.

Current ForceMate Bushing Results

Three specimens were tested with the ForceMate bushings at the interference levels that corresponded to the levels tested on the full scale fatigue test **and** with the EDM pre-flaw at 64.3 degrees. The lives to failure of these specimens are tabulated in Table 2. The average life of the three specimens was approximately 2.5 lifetimes. Also noted in Table 2 are the failure modes, and for specimens B-LL-3, A-UL-2, and A-LL-1, failure occurred from secondary initiated cracks. In other words, crack growth from the pre-flaw at the EDM notch was sufficiently retarded by the compressive residual stresses that naturally initiated cracks were more critical than the induced cracks.

While comparing an average life of 2.5 lifetimes for the original 3 ForceMate specimens to the typical life of 1.0 for the net specimens appears to be an improvement, the location and mode of failure warranted further investigation. Figure 11 is a photograph of the profile of specimen B-LL-3 showing the location of the EDM notch relative to the fracture surface. A photograph of the fracture surface is shown in Figure 12 where multiple initiation sites are marked. Examination of

the bore surface revealed evidence of both fretting and galling, and large deposits of fretting debris collected on the bore surface.

Figure 11 Specimen B-LL-3 after failure, photo on right shows the location of EDM notch relative to fracture face. EDM notch was originally at the 64.3 degrees from the 12:00 location main fracture is a few degrees closer to 6:00.

Examination of the failed specimens B-LL-3, A-UL-2 and A-LL-1 all revealed similar characteristics, namely in all cases, the primary failure initiation was due to internally initiated flaws along the lug bore. That is, in none of the 3 specimens did the flaw initiated from the EDM notch contribute to failure, and all 3 specimens exhibited evidence of both fretting and galling. Fretting debris was present in both the lug bore surface between the bushing and lug. It is postulated that as the fretting debris accumulated between the lug and the bushing, the more aggressive material removal associated with galling occurred.

The specimens B-UK-6 and A-UK-5 also had the forcemate bushing installed at the original interference levels, but these specimens had the EDM notch and pre-flaw clocked to 72 degrees. In the case of these two specimens, failure occurred due to a dominant crack propagating from the pre-crack. The crack length vs life data for these specimens is shown in Figure 10, and the lives to failure are included in Table 2. When the pre-flaw was clocked to 72 degrees, the failure time for the two specimens averaged 1.48 lives (less than the 2.5 average life for the specimens with the flaw at 64.3 degrees).

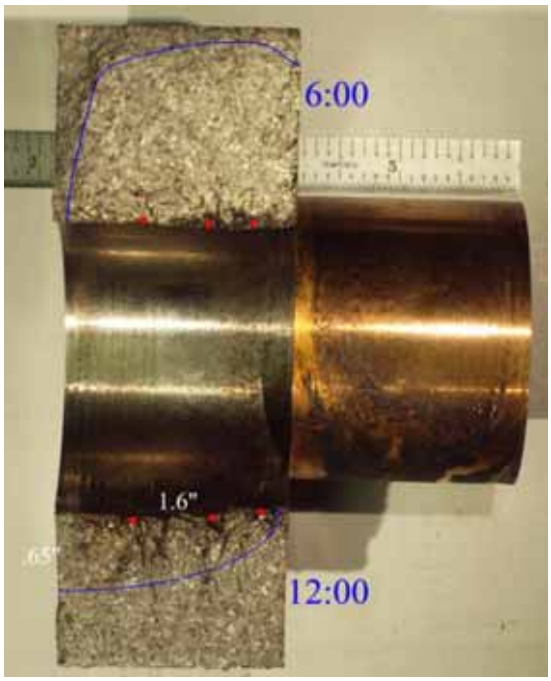

Figure 12 Fracture surface of B-LL-3 showing multiple initiation sites along lug bore. Thin blue lines show the approximate extent of fatigue cracking.

Considered in aggregate, the 5 specimens with the ForceMate bushings at the original expansion level support the following conclusions

- All specimens with ForceMate bushings lasted longer than the specimens with net fit bushings.
- If the crack was not at the precise critical location, failure occurred due to cracking caused by contact fatigue failure modes such as fretting and galling.
- The presence of fretting and galling as contributors to crack nucleation lead to the possibility that the full scale fatigue tests were not an anomaly of the test, but was most likely due to cracking induced by one or both of these contact fatigue mechanisms.

Revised ForceMate bushing results

At the load levels tested,the results that fretting was a significant contributor to crack nucleation suggested that the applied interference levels in the bushing were not sufficient to prevent gapping and relative motion between the lug and bushing This gapping indicated that the applied expansion during installation did not provide sufficient preload for the level of applied stresses and deflections the lug experienced during testing. It was also desirable to eliminate fretting or mitigate its effects to the greatest extent possible.

A bushing that applied a higher level of expansion was designed and installed into two test specimens. The specimen identified as B-LK-7 in Table 1 and Table 2 had this increased expansion bushing installed at the start of the test. This specimen was tested in this configuration for the duration of the test, and. It achieved a life greater than 10 lifetimes. This test configuration is representative of an aircraft lug with this bushing installed “in the factory”. A second specimen, identified as B-UL-4, had a bushing installed to the original configuration for the first 0.5 lifetimes of testing. After 0.5 lifetimes, this bushing was removed and replaced with the increased expansion bushing and testing was continued until 8.9 lifetimes.

Neither of the specimens B-LK-7 nor B-UL-4 failed during spectrum fatigue testing. The crack growth data obtained from B-LK-7 up to 1.5 lifetimes is shown in Figure 10. The significance of this plot is the contrast to the other specimens plotted in this figure. Whereas, each of the other specimens had failed by 2.5 lifetimes the crack in specimen B-LK-7 had grown only to a length of 0.07 inches. The crack length after 10 lifetimes of testing was 0.132 inches, still significantly short of critical crack size.

The long duration of both tests B-LK-7 and B-UL-4 provided confidence that the increased expansion bushing could effectively eliminate fretting as a concern during the aircraft lifetime, and led to the conclusion that increasing the expansion interval on the bushings was a feasible design change to eliminate damage tolerance inspections at these lug bore locations for the anticipated service life and loads.

Experimental Strain Analysis Results

While the long crack growth lives obtained with the increased expansion bushing specimens provided confidence that these bushings provided a solution to the fretting and fatigue issues, the strain gauged specimen described above and shown in Figure 9 provided data to insure that overall residual stresses remained within manageable levels and also provided data with which to benchmark finite element models of the lug test specimens. Table 3 summarizes the strain readings collected from the gages on the outer perimeter of the strain survey specimen shown in Figure 9. The strain values after installation result in residual tension stresses, and the values shown in Table 3 are not large enough to cause concern of tensile failure or secondary initiation sites from the outer edges.

The values in Table 3 shown for the 3:00 position (the tip of the lug), are the lowest in magnitude. However, the lug nose is chamfered and the effect of this chamfer is to create a stress concentration. Figure 13 shows output from a finite element model created to provide additional clarification of the stress state in the test specimen with the increased expansion bushing. Regions of tension stress under applied loading are shown at the bushing on the mandrel entry side. This corresponds to the location where the EDM notch was placed in specimen B-LK-7. The peak hoop stress shown at the lug bore in for this load condition was 46.0 ksi, and the peak stress at the lug nose was 99.7 ksi. Figure 14 is a slightly different view of the finite element analysis contour plots showing how the stress locally peaks at the nose where the section is a minimum due to the chamfer. The chamfer is a necessary design feature to provide clearance into the mating clevis. The necessary tests and analysis to demonstrate that these stress levels did not create a new damage tolerance issue was performed, but is beyond the scope of this current work.

The strain comparison between the FEA and the strain gages on the test lug with the revised bushing are provided in Table 4 and Figure 15. Figure 15 plots the hoop strain as radial distance from the hole edge, and the solid lines plot the strain on the mandrel entry side predicted by the FEM. The dotted lines plot the predicted strain on the mandrel exit side. The data from Table 4 is also plotted onto Figure 15, and three of the four strain gage measurements were within 20% of predicted values. The strain gage labeled number 4 in Table 4 was believed to not be accurate based on other experimental observations, but given the inherent uncertainties in strain measurments of this type, the relative close agreement between analysis and experiment gave confidence in the FEM methods used to model the process.

As a result of the successful agreement between experiment and FEM analysis, additional models were made of the actual aircraft configuration with the ForceMate bushing installed. These models were used to evaluate the actual stress and strain response on the actual aircraft geometry, and these models were in turn used to compute the crack growth life of the lugs.

Table 3 Strain gage readings for gages on outside edge of strain survey specimen

Step Description	Location		
	12:00	3:00	5:00
Test Start	0	0	0
Residual after bush install	1760	1310	1801
Before disconnect	1755	1295	1785
Before Ream (1.981”)	1755	1295	1785
Ream to 2.002"	1730	1273	1748
Ream to 2.004"	1724	1272	1745
Ream to 2.010"	1710	1257	1724
Release Clamps	1706	1257	1722
Before Push out	1755	1295	1785
After Push out	1394	1009	1397

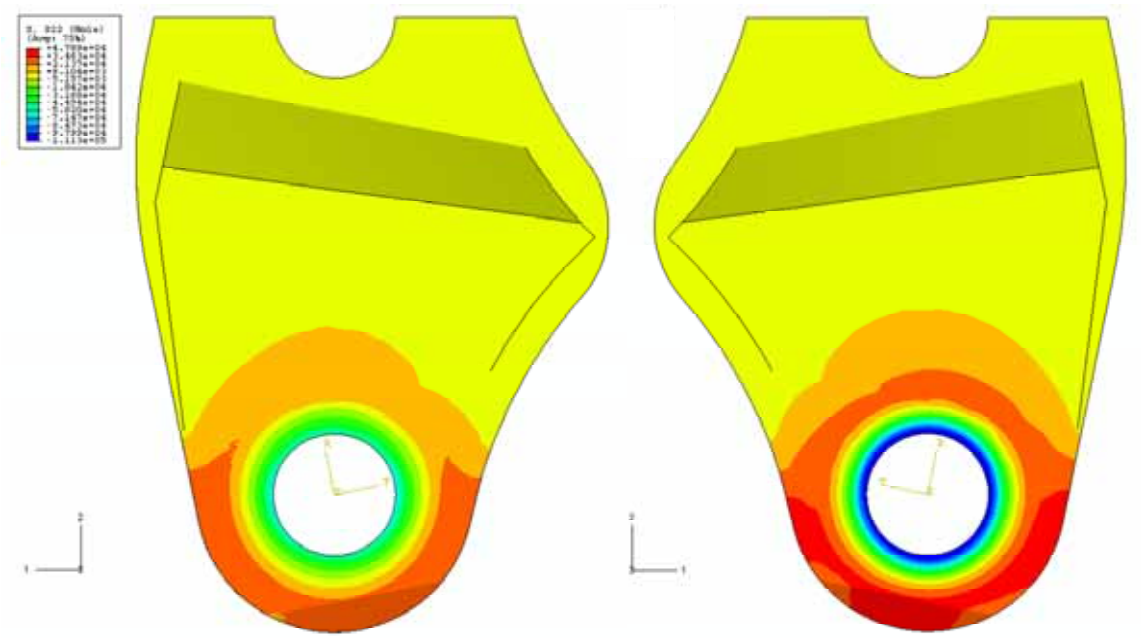

Mandrel Entry Side Mandrel Exit Side

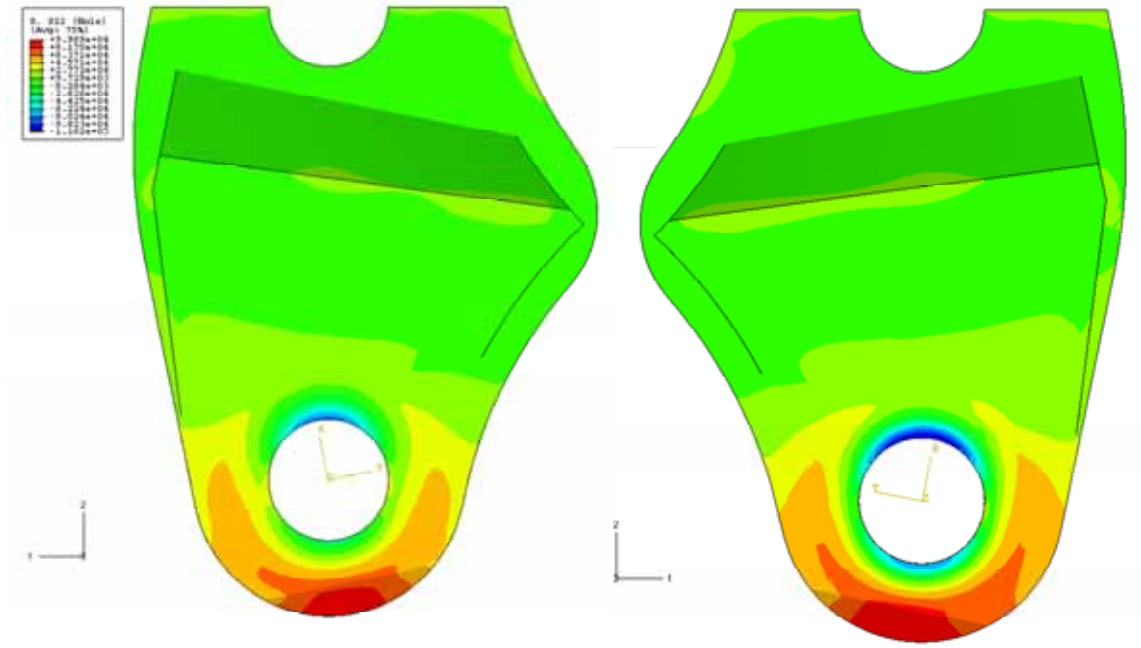

Mandrel Entry Side Mandrel Exit Side

Figure 13 Finite element hoop stress contour plots with the revised bushing installed and 247 kip (1.1 MN) load applied

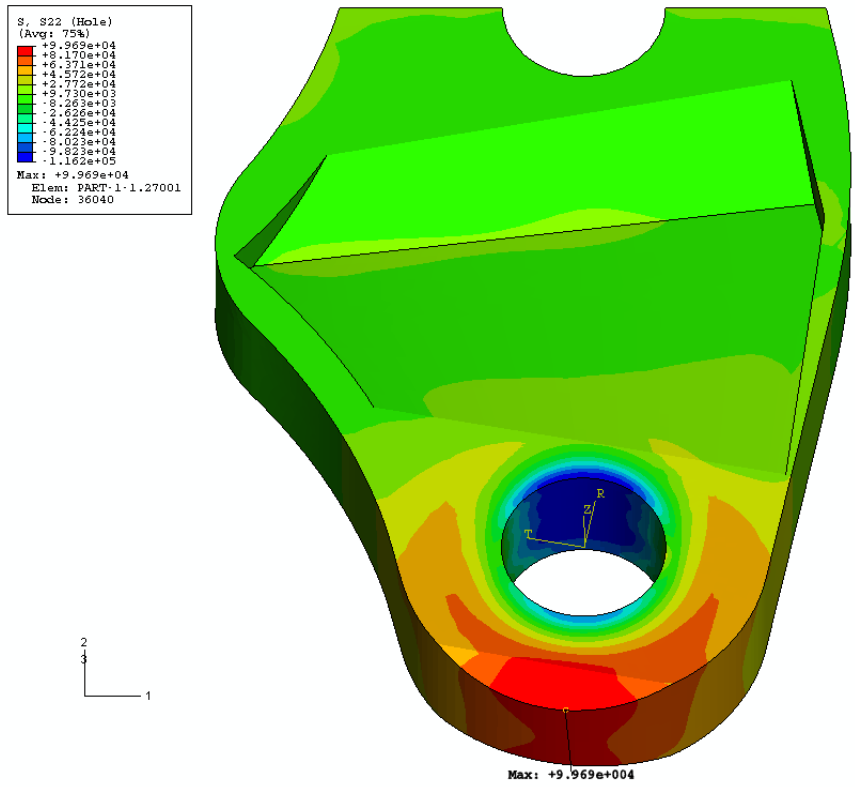

Figure 14 View of contour plot showing peak hoop stress at the lug nose

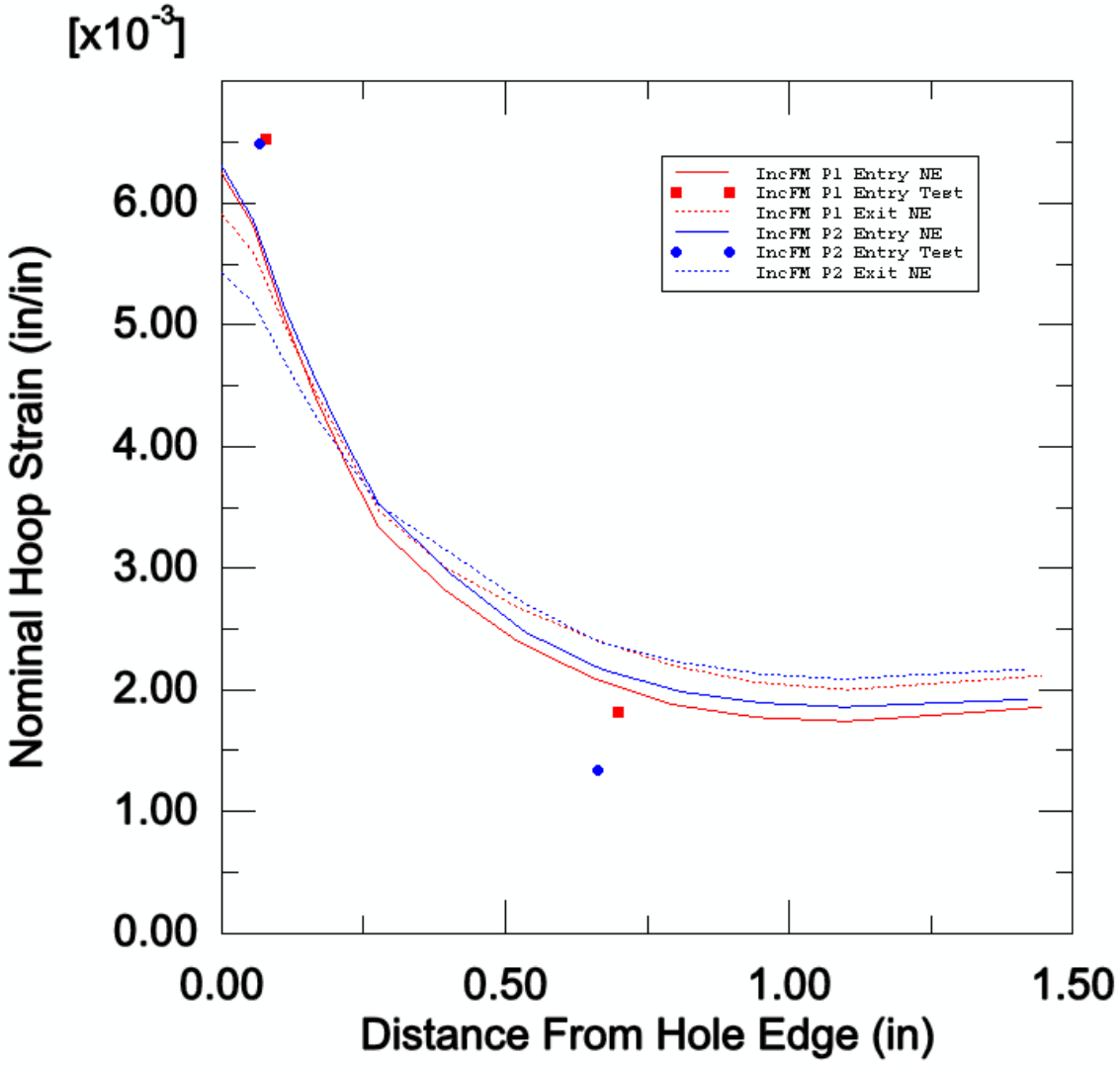

Figure 15 Increased ForceMate Bushing Installed Path Nominal Hoop Strain

Table 4 Increased ForceMate Bushing, Mandrel Entry Side Strain Measurements

Gage Number	Gage Locations	Radial Location (in)	Test Strain (in/in)	FEA Strain (in/in)	Strain Percent Difference
1	5:00	0.0789	0.006529	0.005500	19%
2	5:00	0.6996	0.001818	0.002033	-11%
3	12:00	0.0668	0.006489	0.005722	13%
4	12:00	0.6634	0.001342	0.002185	-39%

Notes:
See Figure 9 for gage locations
Note: Strain percent difference calculated with respect to FEA strain.
The strain values for the Gage Number 4 is suspect based on comparison to Gage Number 2 and Table 3.

Summary and Conclusion

This test program verified the results of the F-22 full scale fatigue test with respect to the cracking of the frame 2 lower lug. This crack was a result of insufficient ForceMate expansion levels for the applied load levels. The increased expansion levels used in this test program verified the solution to the lower lug cracking problem. A design change has been implemented for production aircraft to utilize the bushings at the increased expansion. A program has been proposed to retrofit aircraft that had the original expansion level bushings installed with the increased expansion bushing. Implementation of these design changes and proposed retrofits eliminates the need for further inspections.

References

1. Welsh, S., **Status Of F/A-22 Full Scale Fatigue Test,** Aircraft Structural Integrity Conference (ASIP), 2004

2. Caruso, P., Brussat, T., and Hynes, W. **F-22 Full Scale Durability Test & Evaluation,** Aircraft Structural Integrity Conference (ASIP), 2006.